Author's Accepted Manuscript

www.elsevier.com/locate/talanta

Ultrasensitive sensing of *Androctonus australis hector* scorpion venom toxins in biological fluids using an electrochemical graphene quantum dots/nanobody-based platform

Abdelmoneim Mars, Balkiss Bouhaouala-Zahar, Noureddine Raouafi

PII: S0039-9140(18)30795-1
DOI: https://doi.org/10.1016/j.talanta.2018.07.087
Reference: TAL18916

To appear in: *Talanta*

Received date: 20 April 2018
Revised date: 24 July 2018
Accepted date: 27 July 2018

Cite this article as: Abdelmoneim Mars, Balkiss Bouhaouala-Zahar and Noureddine Raouafi, Ultrasensitive sensing of *Androctonus australis hector* scorpion venom toxins in biological fluids using an electrochemical graphene quantum dots/nanobody-based platform, *Talanta,* https://doi.org/10.1016/j.talanta.2018.07.087

Ultrasensitive sensing of *Androctonus australis hector* scorpion venom toxins in biological fluids using an electrochemical graphene quantum dots/nanobody-based platform

Abdelmoneim Mars,*[1] Balkiss Bouhaouala-Zahar, [2] Noureddine Raouafi[1]

[1] University of Tunis El Manar, Faculty of sciences of Tunis, Laboratory of Analytical Chemistry and Electrochemistry (LR99ES15), Sensors and Biosensors Group, campus universitaire de Tunis El Manar, Tunis El Manar, 2092, Tunis, Tunisia.

[2] University of Tunis El Manar, Institut Pasteur de Tunis, Laboratoire des venins et toxines,

*Corresponding author, E-mail address: A. Mars abdelmoneim.mars@fst.utm.tn

Abstract

Rapid and sensitive detection of low levels of scorpion venom toxins in biological fluids is of tremendous importance for decision-taking in cases of envenomation by scorpions stings. In Tunisia, at least 1200 severe envenomation cases by *Androctonus australis hector* (Aah) scorpion stings were reported annually. In this work, we report on a novel electrochemical immuno-sandwich to detect the Aah50 toxic fraction within the Aah scorpion venom using the bispecific nanobody format specially designed to highly recognize and neutralize the two most toxic molecules in the AahG50 venom fraction (i.e. AahI and AahII toxins), graphene quantum dots (GQDs) constructed on the surface carbon screen-printed electrodes. Hydroquinone/H_2O_2/peroxidase system was used to amplify the current in order to achieve the detection of low levels of AahG50. Electrochemical studies revealed a high sensitivity toward the AahG50 with a sensitivity of 18.2 $nA \cdot mL \cdot pg^{-1}$ and a picomolar limit of detection as low as 0.55 $pg \cdot mL^{-1}$. The platform exhibits very good metrological performances such as repeatability, reproducibility, selectivity and long storage stability. Matrix effect was found to be insignificant as demonstrated by assays performed in human blood serum and urine.

Graphical abstract

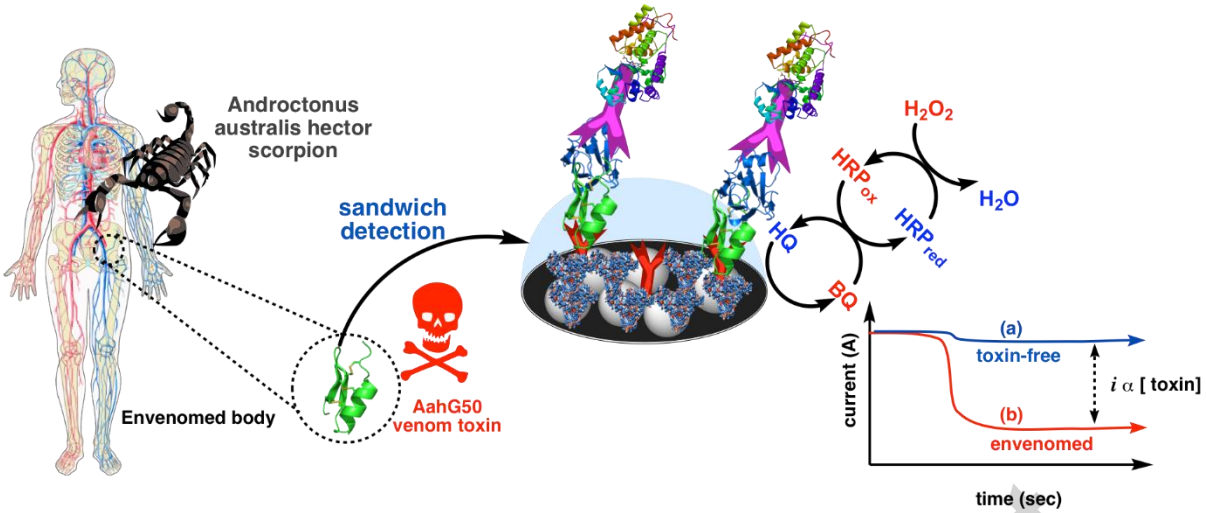

A sensitive electrochemical GQDs/nanobody-based platform for the sensing of AahG50 venom toxins from Androctonus australis hector scorpion stings in biological fluids.

Keywords

Venom toxins; Biosensor; HRP amplification; Nanobody; *Androctonus australis hector*

1. Introduction

Scorpion, spider and snake envenomations are major public health concerns in tropical and subtropical countries especially, Latin America, India, MENA region (i.e. Middle East and North of Africa). World widely, 1 million severe scorpion stings are recorded annually leading to a death toll of 13 500 [1]. More than 200 000 clinical cases are reported annually in Mexico [2] and more than 20 000 cases are claimed in Tunisia, where the Aah scorpion is responsible for most of the recorded fatal stings [3-4]. These statistics forced healthcare scientists to develop rapid and efficient sensing methods to assess the levels of toxicity in order to take the most adequate considerations before medical treatment. Plethora of analytic techniques are routinely used to determine the various toxins present in venoms. For instance, immunofluorescence, MALDI-TOF mass spectrometry, radioimmunoassay, enzyme-linked immunosorbent assay (ELISA), immunodiffusion and ion-sensitive field-effect transistor

(ISFET) are usually employed to detect the toxins. Indeed, Pukrittayakamee *et al.* [5] used a competitive radioimmunoassay to sense Russell's viper venom in fluids victim bodies by developing a monoclonal antibody directed against the factor activator of the venom. The reached detection limit was 4 $ng \cdot mL^{-1}$ in urine and 20 $ng \cdot mL^{-1}$ in 0.1% BSA in phosphate-buffered saline solution. Krifi *et al.* and later on Hammoudi-Triki *et al*. described the use of ELISA to detect antibodies directed to Aah scorpion venom using a double sandwich method [6-7]. Both reported assays used equine polyclonal F(ab')2 and the limit of detection is 0.5 $ng \cdot mL^{-1}$ of venom present in blood serum with a high specificity. Recently, Echterbille *et al.* used MALDI-TOF mass spectrometry to detect and to quantify nAchRs, a toxin from snake venom, by comparing the intensity of the latter in free and in bound fractions extracted from clinical samples [8]. Furthermore, the development of an ISFET-based platform was reported to detect the β-bungarotoxin, present in snake venom [9]. The biosensor can sense toxin level as low as 15.6 $ng \cdot mL^{-1}$. The efficacy of the platform was demonstrated in mouse.

On the other hand, graphene quantum dots (GQDs), as a variety of graphene quantum structures, have become a popular research particle-based nanomaterials making them great candidates in versatile applications such as in photoelectrochemical and photodetection, photovoltaics, optoelectronics and light-emitting diodes (LEDs) and plasmonics [10-20]. Due to the size of GQDs, which is comparable to the Bhor exciton radius, quantum confinement effects became remarkable [21-22].

Variable domains of the heavy chain of a HCAb, called also nanobody (Nb), considered as the smallest antigen binding fragment (approx. MW of 15 kDa) have attracted a lot of interests in biological fields due to the good stability and the high specificity toward target protein [23-25]. Recently, we demonstrated the performance of a bispecific nanobody construct NbF12-10 to recognize and neutralize the whole Aah scorpion venom [26]. In the present work, we combined the GQDs as nanomaterial and the bispecific NbF12-10 nanobody to build a high

sensitive biosensor able to detect the whole toxic fraction AahG50. The main advantage is related to the size of the nanobody which is closely correlated to the scorpion toxins size. Despite, the biosensor used the hydroquinone/H_2O_2/peroxidase for the electrochemical signal amplification in sandwich fashion. The analytical readout was achieved by sampling the current coming from the reduction of BQ, which was produced by the enzymatic digestion of HQ, after forming the immunosandwich at the surface of SPCE. This approach allowed the sensing of at least all venom toxins present in the AahG50 toxic fraction, with a high sensitivity and selectivity. The applicability was also demonstrated in biological fluids.

2. Materials and methods

2.1 Apparatus and electrodes

Electrochemical measurements were recorded using a Metrohm Autolab PGSTAT M204 electrochemical workstation (Basel, Switzerland). Experiments were conducted at room temperature (RT) and data were collected using Nova® v1.11 software. Screen-printed carbon electrodes were purchased from Orion high technologies (Madrid, Spain) consisted of a 4-mm diameter working electrode, a carbon counter electrode and an Ag pseudo-reference electrode.

2.2 Reagents and solutions

All reagents were of the highest available grade. Hydroquinone (HQ), hydrogen peroxide (30%, w/v), PBS tablet (dissolved in 200 mL mQ-water to obtain a 137 mM NaCl, 2.7 mM KCl and 10 mM phosphate buffer solution), 1-ethyl-3-(3-dimethylaminopropyl)carbodiimide (EDC), N-hydroxysuccinimide (NHS), potassium ferricyanide and potassium ferrocyanide were purchased from Sigma-Aldrich (Germany). NbF12-10 nanobody and AahG50 toxic fraction were prepared as previously described [26]. Anti-histidine antibody was purchased from Sigma. Rabbit AahG50-specific polyclonal antibody was prepared and kindly gift by Pr M. El Ayeb, Institut Pasteur Tunis. Lysozyme from chicken egg white, BSA and α-

lactalbumin used as interfering proteins were obtained from Sigma-Aldrich (Germany). Electrochemical impedance spectroscopy (EIS) measurements were carried out using 50 µL of phosphate-buffered saline solution (0.1 mM, pH 7.4) containing a mixture of 5 mM $Fe(CN)_6^{4-}$ and 5 mM of $Fe(CN)_6^{3-}$ as a redox probe. All experiments were run at least on triplicated using different platforms. Only the optimized biosensors providing good analytic performances were used to perform the analysis of the biological samples.

2.3 Graphene quantum dots preparation

Graphene quantum dots were prepared as previously described [27]. Briefly, 2 g of citric acid was heated in a beaker for approximately 20 min at 200 °C until the solution becomes deep orange. After that, 100 mL of 0.1 $mg \cdot mL^{-1}$ NaOH solution was added in the obtained orange liquid. A HCl solution was used (till pH 5.0-6.0) in order to obtain acid carboxylic-terminated GQDs.

2.4 Design of AahG50 immunosandwich

The AahG50 sandwich immunobuilding was achieved using a step-by-step strategy (**Fig.1**). First, the electrode surface was cleaned, by 20 cyclic voltammetry sweeps in 0.5 H_2SO_4, to remove contaminants adsorbed onto carbon surface [28]. A volume of 5 µL GQDs solution was casted on the electrode and left to dry at RT for 3 hours. The anti-AahG50 polyclonal antibody was covalently immobilized through peptide bond between the carboxylic acid from GQDs and amino group of antibodies using EDC/NHS chemistry. The unreacted acid carboxylic groups were blocked with BSA then AahG50 aliquots at different concentrations were casted on the SPCE/GQDs/anti-AahG50 and incubated for 60 min at RT. To form the sandwich, the system was immersed in histidine-tagged NbF12-10 solution (0.1 $\mu g \cdot mL^{-1}$) for additional 60 min. Peroxidase-labelled anti-histidine antibody was added to recognize the

histidine tag. After each step, the electrodes are rinsed thoroughly with ultrapure water and dried under nitrogen.

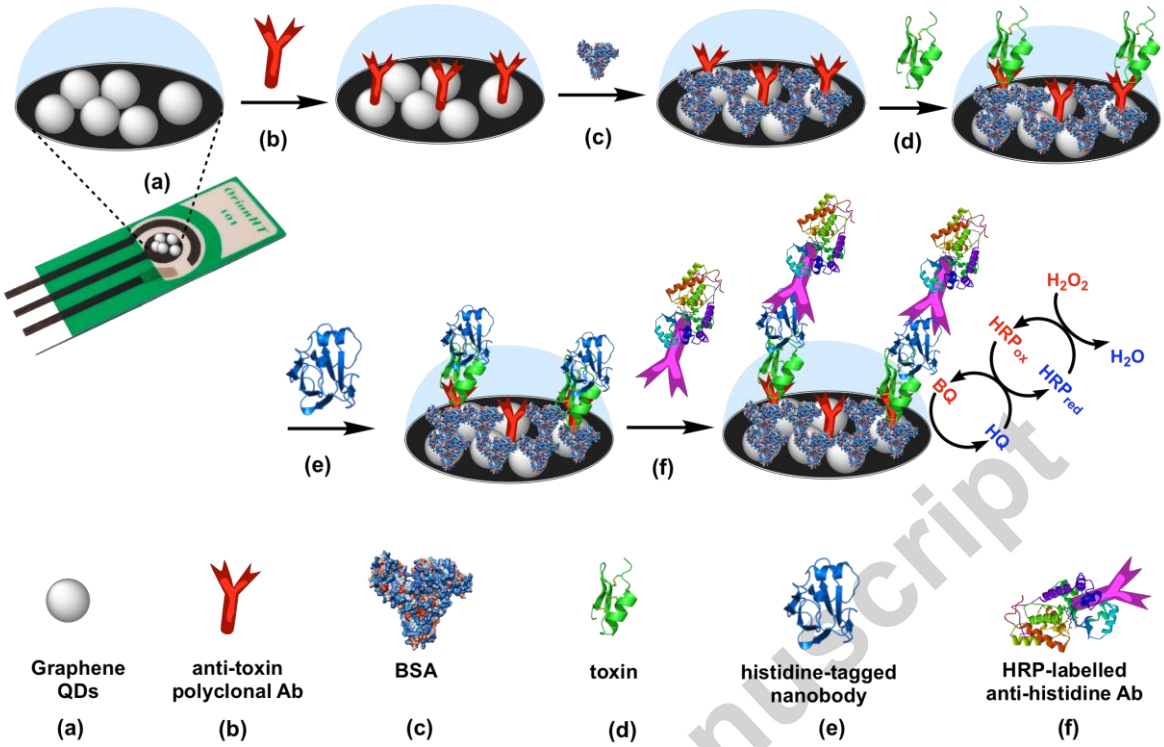

Fig.1 Schematic representation of the stepwise procedure to prepare AahG50 immunosensor

2.4 Amperometric sensing

Amperometric detection was carried out in an electrochemical cell containing 10 mL of 1 mM phosphate buffer saline solution and freshly prepared 1.0 mM HQ solution. The current was sampled at a potential of -0.20 V vs Ag pseudo-reference electrode upon addition of 50 µL of a 0.1 M H_2O_2 solution.

3. Results and discussion

3.1 Characterization of the Aah detection platform

Fluorescence, UV-visible and FTIR spectroscopies were used to characterize graphene quantum dots. Fluorescence and UV-visible spectra showed the presence of a maximum emission and excitation wavelength at 440 and 365 nm, respectively, with the emission of a bright blue light under the excitation with 365 nm UV irradiation (**Fig. 2A and Fig.S1**). FTIR

spectrum reveals the presence of the carboxylic groups on the surface of graphene quantum dots. We noticed two other peaks at 1393 and 1583 cm^{-1} from the carboxylate group and an intense absorption feature centered 2980 cm^{-1} representing C–H bonds (**Fig. 2B**). Typical SEM image of deposed GQDs on the electrode surface, as shown in **Fig. 2C**. Wrinkled GQDs sheets were constructed exhibiting a three-dimensional layered change in carbon electrode. Further, **Inset Fig.2C** provides the TEM image of the GQDs nanomaterials (for full TEM image, see **Fig.S2**). Electrochemical impedance spectroscopy, EIS, which is an ultrasensitive tool, gives information about interfacial features between the electrode surface and electrolyte solution, adsorption process and interactions of recognition biomolecules with electrode surface during the modification steps of AahG50 immunosensor development. **Fig. 2D** presents the impedance plots of stepwise fabrication. Interestingly, the semi-circle diameter decreased considerably after adsorption of GQDs on carbon surface denoting a drastic change in the electron-transfer resistance. This decrement was originated to the conductivity feature of deposed GQDs, which increases the sensitivity of platform due to the great numbers of carboxylic acid on its surface. Before the immobilization of anti-AahG50 polyclonal antibodies, $-CO_2H$ groups were activated by EDC/NHS process inducing a decrease in the electron-transfer resistance. Moreover, EIS Nyquist plots of all other steps, BSA recovery of the non-active acid carboxylic groups, immobilization of antibodies and recognition of nanobodies, showed significant increases in the resistance of the modified surface. These increments are due to the steric hindrance of proteins. In addition, the found EIS values were used to estimate an equivalent circuit model based on Randles model. The fitted equivalent circuit includes a solution resistance (R_s), the charge-transfer resistance (R_{ct}), a Warburg impedance (Z_ω) and the constant phase element (CPE) (**inset Fig.2D**).

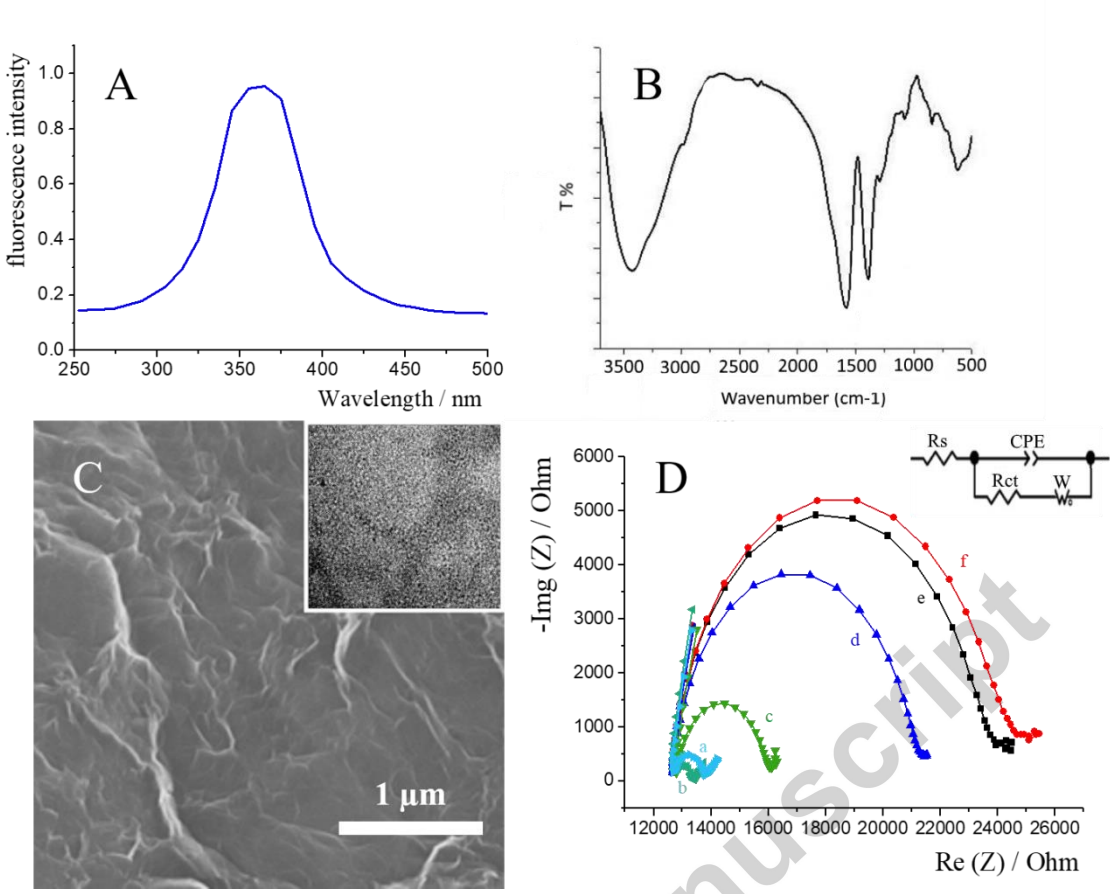

Fig. 2 Fluorescence Spectrum of GQDs (A), FTIR spectra of GQDs (B), SEM image of GQDs modified carbon electrode (inset: TEM image of graphene quantum dots) (C) and EIS Nyquist plots of different steps of modification: bare electrode (a), GQDs modified carbon electrode (b), anti-AahG50-GQDs-SPCE (c), AahG50 toxin-anti-AahG50-GQDs-SPCE (d), histidine AahG50 nanobody-AahG50 toxin-anti-AahG50-GQDs-SPCE (e), HRP-anti.histidine-histidine AahG50 nanobody-AahG50 toxin-anti-AahG50-GQDs-SPCE (f) (D) (For full TEM image of GQDs see S.I).

3.2 Optimization of the experimental variables

Before the sensing process, all relevant experimental variables were optimized as well as a control experiment was performed. The choice of variables has been selected according to the criterion of the highest reduction current obtained at -0.20 V (*vs*. the Ag pseudo-reference electrode) as an applied working potential. This potential was optimized by Zouari *et al*. for HQ/H_2O_2/HRP amplification system in order to detect femtomolar levels of microRNA-21 [29]. The optimization of conditions was summarized in **table 1** (**Fig.S3 and Fig.S4**). The

optimized [poly-anti-AahG50] was found to be 0.1 µg·mL^{-1}. This relatively low value demonstrates that since more target AahG50 toxins would bind on the electrode surface, in a competition assay a high loading density may hinder sensitivity. Furthermore, 0.5% BSA/60 min ratio was chosen as an optimized ratio for blocking agent of non-reacting groups (**Fig.S5 and Fig.S6**). Moreover, the optimal concentration of the used hydroquinone was fixed at 1.0 mM (**Fig.S7**). It is worth to highlight that at low HQ concentration, the current response of the biosensor is very low and limited. The reaction mechanism of the fabricated biosensor can be conclude as follows:

$$H_2O_2 + HRP\ (Red) \rightarrow H_2O + HRP\ (Ox)$$

$$HRP\ (Ox) + HQ\ (Red) \rightarrow HRP\ (Ox) + Q\ (Ox) + H_2O$$

$$Q\ (Ox) + 2e^- + 2H^+ \rightarrow HQ\ (Red)$$

$$= H_2O_2 + 2e^- + 2H^+ \rightarrow 2H_2O$$

Table.1 Optimized experimental variables for the elaboration of AahG50 immunosensor

Experimental variable	Tested range	Selected value
[poly-anti-AahG50], µg·mL^{-1}	0 - 2.0	0.1
Incubation time, h	1 - 6	2
NHS/EDC, mM	1.0 - 10.0	2.0
Incubation time, h	1 - 5	2
Blocking agent BSA, w/v	0 - 3.0	0.5
Incubation time, h	1 - 6	2

In a control experiment, GQDs were removed, and the anti-AahG50 polyclonal was directly attached to the surface through acid carboxylic groups which was formed by electrochemical oxidation of carbon working electrode according to the recently described procedure of Thiagarajan *et al.* [30]. Chronoamperometric studies revealed that a very low reduction current was recorded, denoting the role of GQDs in the signal amplification and improving the sampled current (**Fig.S8**)

3.3 Sensing of AahG50 toxin

Since the toxicity of the Aah scorpion venom is essentially due to the presence of two small basic toxins (i.e. AahI and AahII) having each approximately 7 kDa molecular weight. The anti-AahI/II bispecific nanobody (29 kDa), targeting both most toxic polypeptides of the Aah venom, is ideal for sensitive biorecognition of AahG50 toxic fraction. As shown in **Fig. 3A**, the chronoamperograms of the AahG50-GQDs immunosandwich which were recorded in the presence of different concentrations of the AahG50 revealed a proportional increment in the reduction current with the increase of AahG50 concentration. Dependence of the oxidation current with AahG50 concentrations exhibits a linear response (R^2 = 0.998) from 40 to 700 pg·mL^{-1} (**Fig.3B**). The detection limit was estimated to 0.55 pg·mL^{-1} as expected from the three times standard deviation of the current values obtained for 10 independent amperometric measurements in the absence of AahG50.

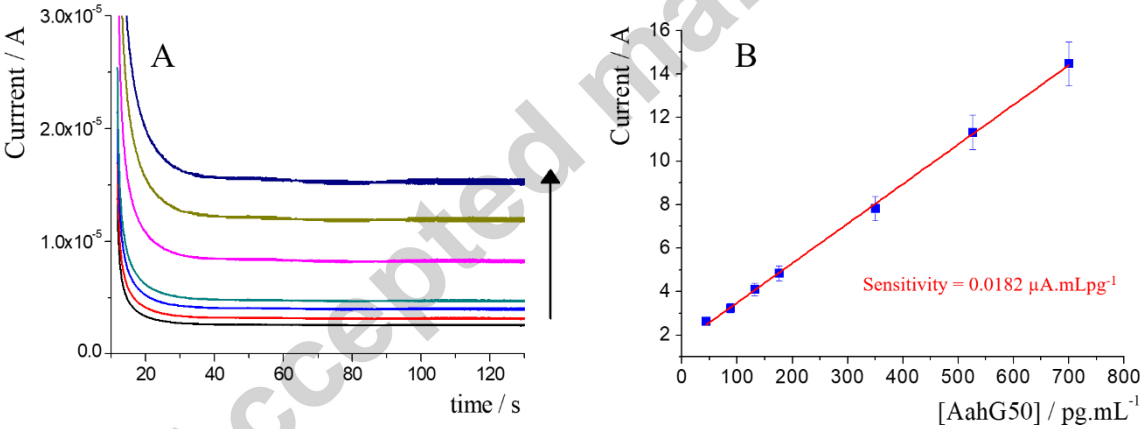

Fig.3 Chronoamperograms of immunosensor with different AahG50 concentrations recorded in hydroquinone/H_2O_2 solution (A) and the corresponding calibration plot (B). Recorded applied potential at -0.2 V *Vs* Ag pseudo-reference electrode.

3.4 Analytic performances

3.4.1 Repeatability, reproducibility and storage stability

The repeatability of one electrode was studied by measuring the oxidation current induced by the recognition of 90 pg·mL^{-1} of AahG50 toxins for 20 times in a one single day. The relative

standard deviation (RSD) was found to be 2.8%. Moreover, the electrode-to-electrode reproducibility was determined by interpreting the sampled current from six different AahG50 immunosandwich formed with the same amount of venom toxic fractions. The platform showed a high reproducibility with a 3.6% RSD value. Furthermore, three electrodes, which showed the best reproducibility, were stored in the fridge at 4 °C for one month. Daily recorded chronoamperograms revealed a decrease by only 6.0%, indicating the great stability of the platforms. All these results are in favor of the positive impact of the biological-nanomaterial matrix, nanobody- GQDs (**Fig. S9**).

3.4.2 Interference study and detection of AahG50 in urine and human serum

Because of their low molecular weights, lysozyme (16.5 kDa) and α-lactalbumin (14.2 kDa) were chosen as interfering proteins to challenge the response of the platform toward AahG50. Selectivity was investigated by comparing amperometric responses of the immunosandwich in the presence of the AahG50, AahG50 and lysozyme or AahG50 and α-lactalbumin. **Fig. 4A** displays the amperometric curves of the selectivity experiments. As expected, the response observed with the immunosandwich built in presence AahG50 and the interfering proteins, did not show any notable changes when compared to what obtained with AahG50 alone, denoting a high selectivity of the method. Moreover, we studied amperometric response of AahG50 immunosandwich in clinical fluids such as urine and human blood serum to assess the effect of the complex matrices. Chronoamperograms recorded in serum and urine revealed a high sensitivity of response around 15.32 and 13.97 $nA \cdot pg \cdot mL^{-1}$, respectively. These values of sensitivity are very close to those obtained with the AahG50 in PBS and confirm the suitability of this platform to sense AahG50 toxic fraction directly in sera and urine samples (**Fig.4B and Fig. S10**).

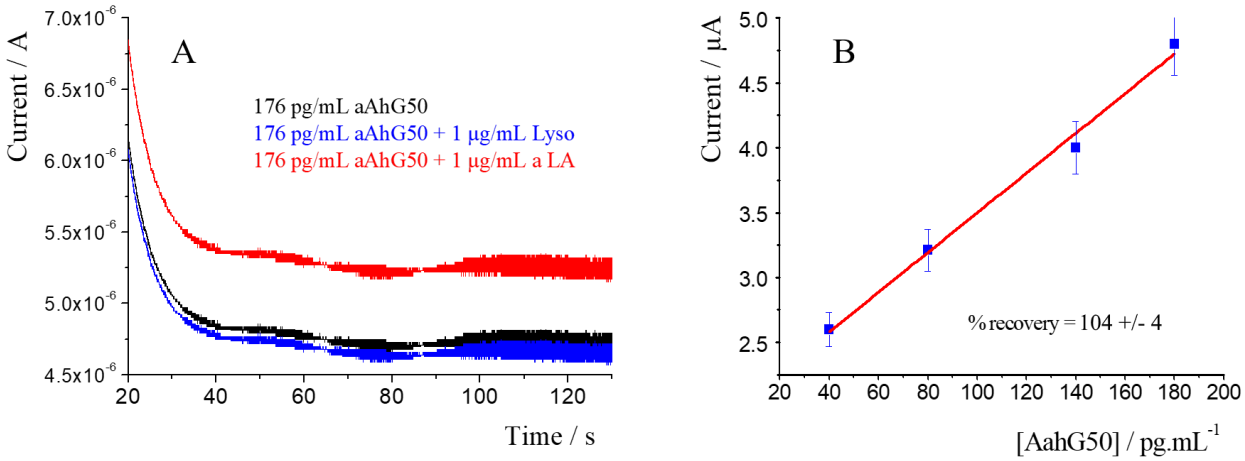

Fig.4 Chronoamperograms of selectivity experiments in the presence of lysozyme and α-lactalbumin (A) and correlation curve of recorded chronoamperograms in human blood serum (B).

3.4.3 Comparative study

To evaluate the as-developed biosensor, we compared its performances with other methods developed for the sensing of venom toxins. It is worth mentioning that we did not find until today any amperometric biosensors designed to detect venoms especially from scorpion species (**Table.2**). The reported biosensor has a much lower limit of detection especially that the amounts of venom toxins are very low because the scorpion stings introduced a few dozen of microliter of venom in 4 to 5 litres of circulating blood. Furthermore, the biosensor has an acceptable linear range.

Table.2 Summary of works reporting toxins venom biosensing techniques.

Techniques	Predators Toxins	LOD	References
ELISA	*Androctonus australis Hector* scorpion	0.5 ng/mL	Krifi *et al.*, 1998 [6]
ELISA[a]	*Tityus serrulatus* scorpion	0.1 ng/mL	Chávez-Olórtegui et al., 1994 [31]
Fluorimetry	Paralytic shellfish toxin	1 ng/mL	Louzao et al., 2001 [32]
ISFET	β-bungarotoxin of *Bungarus*	15.6 ng/mL	Selvanayagam et al., 2002 [9]
LC-Fluorescence[b]	Palytoxin-like of *ostreopsis*	0.75 ng/mL	Riobo et al., 2006 [33]

competitive RIA[c]	Russell's viper toxin	20 ng/mL	Pukrittayakamee et al., 1987 [5]
Amperometry	AahG50 toxin	0.55 pg/mL	Present work

[a]ELISA: enzyme-linked immunoassay, [b]LC: liquid chromatography, [c]RIA: radioimmunoassay

4. Conclusion

To the best of our knowledge, we report in this paper the design of the first case of an amperometric biosensor to detect scorpion venom toxins displaying rapid body diffusion. The sensitive and robust sensing platform is built by combining the unique features of graphene quantum dots and the high selectivity of the best in class nanobody candidate (NbF12-10) generated to fight scorpion envenomation. Hydroquinone/H_2O_2/peroxidase system was used to amplify electrochemical signal allowing the sensing of the toxic fraction AahG50 in pg/mL range. Using this platform, the scorpion toxins can be detected in human serum blood and urine with a minimal interference from the matrices. Storage stability, repeatability and reproducibility experiments confirmed the feasibility of the system to perform accurate determination of the target toxins. The same principle can be expended to develop new platforms for the other venom fractions from different animal species. The platform miniaturization will allow using the biosensing of AahG50 main toxic fraction and therefore scorpion envenomings in primary healthcare centers.

Acknowledgements

Authors wish to acknowledge the financial support from LVMT and LCAE laboratories funded by the Ministry of High Education and Scientific research and the NanoFastResponse PRF2017-D4P1 national and federative project.

References

[1] J.P. Chippaux, M. Goyffon, Epidemiology of scorpionism: a global appraisal, Acta Trop. 107 (2008) 71-79.

[2] M. Dehesa-Davila, L.D. Possani, Scorpionism and serotherapy in Mexico, Toxicon 32 (1994) 1015–1018.

[3] M. Goyffon, M. Vachon, N. Broglio, Epidemiological and clinical characteristics of the scorpion envenomation in Tunisia, Toxicon 20 (1982) 337–344.

[4] M. Bouaziz, M. Bahloul, H. Kallel, M. Samet, H. Ksibi, H. Dammak, M. N. Ben Ahmed, K. Chtara, H. Chelly, C. Ben Hmida, N. Rekik, Epidemiological, clinical characteristics and outcome of severe scorpion envenomation in South Tunisia: Multivariate analysis of 951 cases

Toxicon 52 (2008) 918-926.

[5] S. Purittayakamee, P.J. Ratcliffe, A.J. McMichael, D.A. Warrell, D. Bunnag, A competitve radioimmunoassay using a monoclonal antibody to detect the factor X activator of Russell's viper venom, Toxicon 25 (1987) 721-729.

[6] M. N. Krifi, N. Marrakchi, M. El-Ayeb, K. Dellagi, Effect of some variables on the in vivo determination of scorpion and viper venom toxicities, Biologicals 26 (1998) 277-288

[7] D. Hammoudi-Truki, F. Laraba-Djebari, Application of ELISA for the quantification of Androctonus austalis hector venom in the envenomed serum of people and rats before and after immunotherapy, Bull. Soc. Pathol. Exot. 96 (2003) 297-301.

[8] J. Echterbille, N. Gilles, R. Araoz, E. De Pauw, L. Quinton, Methodology to fish peptide ligands of nAChRs from Cone snail venoms by MALDI-TOF mass spectrometry, ORBI. (2016).

[9] Z.E. Selvanayagam, P. Neuzil, P. Gopalakrishnakone, U. Sridhar, M. Singh, L.C. Ho, An ISFET-based immunosensor for the detection of β-Bungarotoxin, Biosens. Bioelectron. 17 (2002) 821-826.

[10] L. Tang, R. Ji, X. Li, G. Bai, C.P. Liu, J. Hao, J. Lin, H. Jiang, K. S. Teng, Z. Yang , S. P. Lau, Deep Ultraviolet to near-infrared emission and photoresponse in layered N-doped graphene quantum dots, ACS Nano. 8 (2014) 6312-6320.

[11] Q. Zhang, J. Jie, S. Diao, Z. Shao, Q. Zhang, L. Wang, W. Deng, W. Hu, H. Xia, X. Yuan, S. T. Lee, Solution-processed graphene quantum dot deep-UV photodetectors, ACS Nano. 9 (2015) 1561-1570.

[12] Y. Li, Y. Hu, Y. Zhao, G. Shi, L. Deng, Y. Hou, L. Qu, An electrochemical avenue to green-luminescent graphene quantum dots as potential electron-acceptors for photovoltaics Adv Mater. 23 (2011) 776-780.

[13] X. M. Li, M. C. Rui, J. Z. Song, Z. H. shen, H. B. Zeng, Carbon and graphene quantum dots for optoelectronic and energy devices: A review, Adv. Funct. Mater. 25 (2015) 4929-4947.

[14] V. Gupta, N. Chaudhary, R. Srivastava, G. D. Sharma, R. Bhardwaj, S. Chand, Luminescent graphene quantum dots for organic photovoltaic devices, J. Am. Chem. Soc. 133 (2011) 9960-9963.

[15] C. M. Luk, L. B. Tang, W. F. Zhang, S. F. Yu, K. S. Teng, S. P. Lua, An efficient and stable fluorescent graphene quantum dot-agar composite as a converting material in white light emitting diodes, J. Mater. Chem. 22 (2012) 22378-22381.

[16] Z. Fei, A. S. Rodin, G. O. Andreev, W. Bao, A. S. Mcleod, M. Wagner, L. M. Zhang, Z. Zhao, M. Thiemens, G. Dominguez, M. M. Fogler, A. H. Castro Neto, C. N. Lau, F. Keilmann, D. N. Basov, Gate-tuning of graphene plasmons revealed by infrared nano-imaging, Nature 487 (2012) 82-85.

[17] W. Gao, J. Shu, C. Qui, Q. Xu, Excitation of plasmonics waves in graphene by guided-mode resonances, ACS. Nano. 6 (2012) 7806-7813.

[18] X. Li, Y. Wang, L. Shi, H. Ma, Y. Zhang, B. Du, D. Wu, Q. Wei, A novel ECL biosensor for the detection of concanavalin A based on glucose functionalized NiCo2S4 nanoparticles-grown on carboxylic graphene as quenching probe, Biosens. Bioelectron. 96 (2017) 113-120.

[19] X. Wang, R. Xu, X. Sun, Y. Wang, X. Ren, B. Du, D. Wu, Q. Wei, Using reduced graphene oxide-Ca:CdSe nanocomposite to enhance photoelectrochemical activity of gold nanoparticles functionalized tungsten oxide for highly sensitive prostate specific antigen detection, Biosens. Bioelectron. 96 (2017) 239-245.

[20] X. Li, S. Yu, T. Yan, Y. Zhang, B. Du, D. Wu, Q. Wei, A sensitive electrochemiluminescence immunosensor based on $Ru(bpy)_3^{2+}$ in 3D CuNi oxalate as luminophores and graphene oxide–polyethylenimine as released $Ru(bpy)_3^{2+}$ initiator, Biosens. Bioelectron. 89 (2017) 1020-1025.

[21] F. Sols, F. Guinea, A. H. Neto, Effect of Electron Interaction on Statistics of Conductance Oscillations in Open Quantum Dots: Does the Dephasing Time Saturate?, Phys. Rev. Lett. 99 (2007) 1-4.

[22] Q. Zhang, X. Li, M. M. Hossain, Y. Xue, J. Zhang, J. song, J. Liu, M. D. turner, S. Fans, M. Gu, Graphene surface plasmons at the near-infrared optical regime, Sci. Rep. 4 (2014) 1-6.

[23] T. N. Baral, S. Magez, B. Stijlemans, K. Conrath, B. Vanhollebeke, E. Pays, S. Muyldermans, P. De Baetselier, Experimental therapy of African trypanosomiasis with a nanobodyconjugated human trypanolytic factor, Med. Sci. 22 (2006) 914–916.

[24] V. Cortez-Retamozo, N. Backmann, P. D. Senter, U. Wernery, P. De Baetselier, S. Muyldermans, H. Revets, Efficient targeting of conserved cryptic epitopes of infectious agents by single domain antibodies, J. Biol. Chem. 279 (2004) 1256–1261.

[25] X. Ren, J. Yan, D. Wu, Q. Wei, Y. Wan, Nanobody-Based Apolipoprotein E Immunosensor for Point-of-Care Testing, ACS Sens. 2 (2017) 1267-1271.

[26] I. Hmila, D. Saerens, R. Ben Abderrazek, C. Vincke, N. Abidi, Z. Benlasfar, J. Govaert, M. El-Ayeb, B. Bouhaouala-Zahar, S. Muyldermans, A bispecific nanobody to provide full protection against lethal scorpion envenoming, FASEB J. 24 (2010) 3479-3489.

[27] M. Roushani, Z. Abdi, Novel electrochemical sensor based on graphene quantum dots/riboflavin nanocomposite for the detection of persulfate, Sensor. Actuat. B-Chem. 201 (2014) 503-510.

[28] J. Wang, M. Pedrero, H. Sakslund, O. Hammerich, J. Pingarron, Electrochemical activation of screen-printed carbon strips, Analyst 121 (1996) 345-350.

[29] M. Zouari, S. Campuzano, J. M. Pingarron, N. Raouafi, Competitive RNA-RNA hybridization-based integrated nanostructured-disposable electrode for highly sensitive determination of miRNAs in cancer cells, Biosens. Bioelectron. 91 (2017) 40-45.

[30] S. Thiagarajan, T. H. Tsai, S. M. Chen, Easy modification of glassy carbon electrode for simultaneous determination of ascorbic acid, dopamine and uric acid, Biosens. Bioelectron. 24 (2009) 2712-2715.

[31] C. Chavez-Olortegui, S. Carolina, G. Fonseca, D. Campolina, A. R. Faria Santos, C. Diniz, ELISA for the detection of toxic antigens in experimental and clinical envenoming by *Tityus serrulatus* scorpion venom, Toxicon 32 (1994) 1649-1656.

[32] M. C. Louzao, M. R. Vieytes, J. M. V. Baptista de Sousa, F. Leira, L. M. Botana, A fluorimetric method based on changes in membrane potential for screening paralytic shellfish toxins in mussels, Anal. Biochem. 289 (2001) 246-250.

[33] P. Riobo, B. Paz, J. M. Franco, Analysis of palytoxin-like in ostreopsis cultures by liquid chromatography with precolumn derivatization and fluorescence detection, Anal. Chim. Acta. 566 (2006) 217-223.

Highlights

- A sensitive amperometric immunosandwich nanobody sensor was developed.
- The sensing performance for venom toxin was monitored by Hydroquinone/H_2O_2/peroxidase system.
- The Limit of detection was founded to be 0.55 pg.mL^{-1} with a sensitivity of 18.2 nA.mL.pg^{-1}.
- A good metrological performances was demonstrated such as repeatability, reproducibility and storage test.
- Human blood serum and urine were used as real matrix.